From Lab to Industrial:

PZT nanoparticles synthesis and process control for application in additive manufacturing

Hsien-Lin Huang

A thesis

Submitted in partial fulfillment of the

Requirements for the degree of

Master of Science

University of Washington

2013

Reading Committee:

I-Yeu (Steve) Shen, Chair

Guozhong Cao, Co-Chair

Scott Johnston

Program Authorized to Offer Degree:

Mechanical Engineering

Contents

List of Figures

List of Tables

Abstract

Lead Zirconate Titanate (PZT) nanoparticles hold many promising current and future applications, such as PZT ink for 3-D printing or seeds for PZT thick films. One common method is hydrothermal growth, in which temperature, duration time, or mineralizer concentrations are optimized to produce PZT nanoparticles with desired morphology, controlled size and size distribution. A modified hydrothermal process is used to fabricate PZT nanoparticles. The novelty is to employ a high ramping rate (e.g., 20˚C/min) to generate abrupt supersaturation so as to promote burst nucleation of PZT nanoparticles as well as a fast cooling rate (e.g., 5˚C/min) with a controlled termination of crystal growth. As a result, PZT nanoparticles with a size distribution ranging from 200 nm to 800 nm are obtained with cubic morphology and good crystallinity. The identification of nanoparticles is confirmed through use of X-ray diffractometer (XRD). XRD patterns are used to compare sample variations in their microstructures such as lattice parameter. A cubic morphology and particle size are also examined via SEM images. The hydrothermal process is further modified with excess lead (from 20% wt. to 80% wt.) to significantly reduce amorphous phase and agglomeration of the PZT nanoparticles. With a modified process, the particle size still remains within the 200 nm to 800 nm. Also, the crystal structures (microstructure) of the samples show little variations. Finally, a semi-continuous hydrothermal manufacturing process was developed to substantially reduce the fabrication time and maintained the same high quality as the nanoparticles prepared in an earlier stage. In this semi-continuous process, a furnace is maintained at the process temperature (200˚C), whereas autoclaves containing PZT sol are placed in and out of the furnace to control the ramp-up and cooling rates. This setup eliminates an extremely time-consuming step of

cooling down the furnace, thus saving tremendous amount of process time making fabrication of a large amount of PZT nanoparticles possible.

Acknowledgement

My appreciation to my advisors, Professor Shen, from Mechanical Engineering department and Professor Cao, from Material Engineering department, cannot be described in few words. Their knowledge, patience, guidance, and inspiration strengthen me, in both academic and personal life. They also helped me to understand my weakness and gained me ways to improve it.

I also want to thank Dr. Scott Johnston and Mr. Jeff Duce, from the Boeing Company. Without their support, this project could not be completed. Working with them has helped me to gain experience on industrial perspectives

A special acknowledgement should be addressed to Mechanical Engineering department staff—Maria Hooper, the graduate student advisor, Wanwisa Kisalang, the program Coordinator, Nancy Moses, the Administrative Coordinator. Their patience and warmth on helping me made me feel that I am connected with ME personally.

Least, but the last, I want to thank all my mentors and colleagues—Qing Guo, Chuan Luo, Ya-Fang Cheng, Wei-Chi Tai, and Robert Manson. I did not have a mechanical engineering background and they are always welling to help me on all kinds of questions I have, such as operation on matlab, solving a dynamic problem or an engineering math problem, and more. They made me feel that I am home and I have learned a lot from each of them.

Without all of their courage and support, I would not be able to make this far. The learning process continues with all the lessons I received from them.

Chapter 1
General Introduction

1.1 Overview

Lead Zirconate Titanate (PZT) nanoparticles, granules, or powder hold many promising current and future applications. For example, PZT powder can be suspended in solvent to form PZT ink for 3-D printing [1-5]. PZT nanoparticles can also be suspended in PZT sol to serve as seeds to lower sintering temperature of sol-gel derived PZT films [3]. PZT in granular forms can be pressed and sintered into specific shapes, such as disks and benders [6]. PZT nanoparticles can be embedded in silica matrix to form sensors and actuators [5,7,8].

To enable these applications, the first task is to have a large quantity of high-quality PZT nanoparticles. The nanoparticles must have narrow size distribution. Moreover, the size of the nanoparticles should be relatively insensitive to fabrication parameters. The size of the particles must be large enough (e.g., > 200 nm) to ensure good piezoelectric properties. On the other hand, the size of the nanoparticles cannot be too large (e.g., < 1 μm); otherwise, they may precipitate in PZT ink fabrication or clog 3-D printer nozzles. The PZT nanoparticles should have accurate stoichiometric composition, uniform morphology, and proper microstructures to ensure good piezoelectric properties. Since a large quantity of PZT nanoparticles is needed, the fabrication process must be simple and easy to control in order to achieve a high production rate.

Currently, there are two common approaches to make PZT nanoparticles. The first way is a top-down approach often used in the industry [6,9]. In this approach, a large amount of PZT aggregates is fabricated by calcination and then milled down to the desired size. There are several major problems. First, the particles of PZT are damaged during the milling process resulting in non-uniform particle morphology; see Figure 1. Second, the size and morphology of PZT particles vary widely. As shown in Figure 1, particle size can be somewhere from 500 nm to couple hundred micron. Also, contaminates are often introduced during the milling process. Therefore, the top-down approach does not generate high-quality PZT particles with good piezoelectric performance [10].

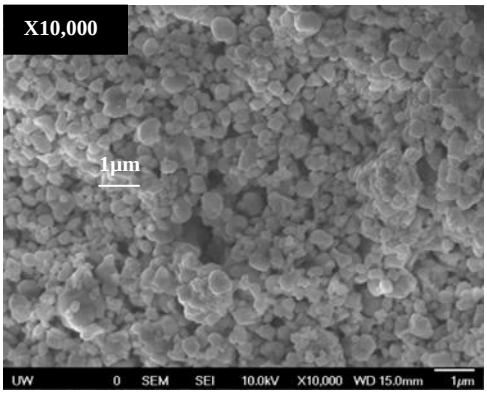

Figure 1 SEM image of PZT particles from a top-down approach (X10,000)

The second method is a bottom-up approach that is still under active investigation in various research communities. In this approach, PZT particles are grown and prefabricated from sol via a hydrothermal process, for example [11-17]. Size and quality of PZT nanoparticles are controlled by various process parameters, such as temperature, time, and mineralizer concentration [11-15,17].

Although these hydrothermal processes have successfully resulted in functional PZT nanoparticles, they are not readily translational to real applications for several reasons. Some fabricated PZT particles do not have the desirable size (e.g., 5 µm for Harada et al. [14] and 25

nm for Das et al. [16]). Other fabricated PZT nanoparticles heavily rely on mineralizer concentration to control the particle size. As a result, the particle size is very sensitive to mineralizer concentration and a uniform particle size becomes difficult to achieve [11, 13, 15]. In some cases, the process time is as long as 24 hours with long ramp-up and cool-off periods [13]. There is a strong need for a new hydrothermal process that is fast and easy to control the resulting particle size.

1.2 Piezoelectric materials

1.2.1 General introduction

Piezoelectric material belongs to the dielectric material family which changes dimension upon application of an external electric field. The dielectric material can be further divided into two sub-groups—centrosymmetric class and noncentrosymmetric class. Centrosymmetric class represents non-piezoelectric dielectric materials and the dimension change under the external electric field is small. On the other hand, the noncentrosymmetric class has more significant dimension changes under the external applied electric field compared to the centrosymmetric dielectric materials due to its asymmetric movement of the adjacent ions. The resulting strain, which can be either extensive or compressive, is directly proportional to the applied external electric field. In addition, piezoelectric material has a unique property of generating an induced electric field under an external strain by an applied stress. [18]

Piezoelectric materials can be further divided into non-pyroelectric and pyroelectric.

For pyroelectric material, temperature affects spontaneous polarization. Non-ferroelectric and ferroelectric are the sub classes of the pyroelectric materials. The difference between non-ferroelectric and ferroelectric materials is that ferroelectric materials have the ability to reverse or to re-orient the spontaneous polarization by an external electric field after the spontaneous polarization decreases. In general, ferroelectric materials have better piezoelectric and pyroelectric characteristics than non-ferroelectric materials [18].

1.2.2 Lead Zirconcate Titanate (PZT)

Some of the commonly used piezoelectric materials include quartz, Lead Zirconcate Titanate (PZT), Polyvinylidene Flouride (PVDF), Barium Titanate, Zinc Oxide, and…etc. Among these piezoelectric materials, PZT is one of the most known and studied piezoelectric material due to its excellent piezoelectric and mechanical properties. The chemical formula of PZT is $PbZr_xTi_{1-x}O_3$ which is a solid solution of lead zirconate ($PbZrO_3$), and lead titanate ($PbTiO_3$). The value of "X" depends on the percentage of lead zirconate. PZT has perovskite crystal structure, which its unit cell structure is shown in Figure 2. The unit cell has one molecule of lead atom is contained in at the corner (1/8 atom at each corner), three oxygen atoms at the face centres (1/2 atom at each face), and one zirconium or titanium at the center of the unit cell.

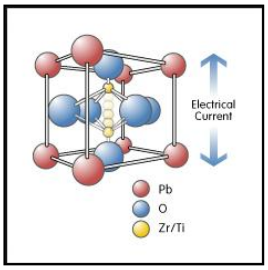

Figure 2 Unit cell structure of PZT

Phase diagram of PZT is shown in Figure 3 PZT Phase diagram Above Curie temperature (Pc

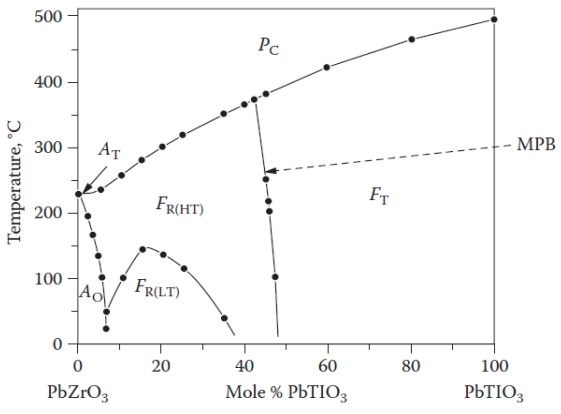

Figure 3 PZT Phase diagram

region), PZT appears to be paraelectric and has cubic crystal structure. Below Curie temperature with $PbTiO_3$ content greater than 5%, PZT appears to be ferroelectric, which has great piezoelectric properties among the dielectric materials. In addition, under Curie temperature, the $PbTiO_3$ phase has crystal structure as tetragonal and it has 6 easy polarization directions along <100> orientation, and the PbZrO3 phase has crystal structure as rhombohedral and it has 8 easy polarization directions along <111> orientation. Along the morphotropic phase boundary, PZT has 52% of $PbZrO_3$ and 48% $PbTiO_3$, both $PbTiO_3$ and $PbZrO_3$ poised between these two structures with equal probability and has 14 total easy polarization directions. Therefore, PZT with this specific composition has the highest piezoelectric coefficient d_{33} and dielectric constant along MPB.

1.3 Fabrication of PZT particles

There are three commonly used techniques for fabrication of PZT particles—solid-state reaction, coprecipitation, and sol-gel techniques.

In solid-state technique, a proper molar ratio of oxides is mixed and then undergoes solid-state reaction by a calcination process, which is a top down method introduced in the beginning of the chapter. The calcination processes the oxides under around 650˚C for 2 to 3 hours and then is held under around 850˚C to allow recrystallization. The final product is milled down to desired particle size. The typical resulting PZT particle size is around 1μm [18].

The second technique is co-precipitation from solution [18], which is the method used throughout this study. Precipitates which are formed by mixing an aqueous solution of oxides

with proper molar ratio with a precipitating agent. Then, the precipitates are filtered and undergo a thermal process to form a desired product—PZT in this case. Hydrothermal process is one of the typical coprecipitation techniques. The important parameters include pH of the solution, mixing rate, ratio of the oxides, and temperature. With proper adjustment of the parameters, the resulting PZT can achieve high purity and fine particles. Particle size can be few nanometers to few microns depended on parameter set up.

Third common technique—sol-gel process uses polymerization reaction of soluble precursor compounds to create three dimensional structures and form gel [18]. The gel is dried and grounded. It creates PZT with high purity and high density. However, the downside is that the raw materials of sol-gel methods are generally more expensive than other two techniques.

Both second and third techniques are bottom up methods and can produce high purity PZT. The work in this thesis is focusing on the second technique—coprecipitation rather than the sol-gel technique due to the following two reasons. One is cost effectiveness. As mentioned earlier, the raw material used in sol-gel is more expensive and high firing temperature, which is not desirable for manufacturing purpose. The other reason is that sol-gel technique still involves grounding since the gel was directly fired and formed polycrystals and this may lead to the same problems—contamination and non-uniform morphology as the solid-state technique.

1.4 Research Objective

Based on the introduction, there is a demand to develop a process that having both high production rate and high quality of PZT nanoparticles for applications in manufacture. Even though in Lab scale, the production rate cannot compete with manufacturing scale, demonstration of possibility in increasing production rate and producing high quality of PZT nanparticles is the first step to scale up for development in manufacturing process. The research involves three stages. During the first stage, the object was to develop an alternative method of control particle size and morphology. The study began with a parametric study to determine a proper processing time is needed for PZT formation with certain choices of mineraliser concentration under 200˚C for hydrothermal growth. After the parameters of mineraliser concentrations and co-responding growth times were known, ramping rates and cooling rates were added into the process control to alter the quality of PZT nanoparticles. The objective in second stage was to refine the quality of the PZT nanoparticle. With controlling ramping and cooling rates, cubic morphology and particle size between 200 nm to 800 nm was achieved. However, the best scenarios have challenges as large amount of amorphous phase and severe degree of agglomeration. Amorphous phase will reduce the overall piezoelectric properties. Severe agglomerated PZT nanoparticles have no practical use. Therefore, they need to be removed or reduced. Fine tune in morphology and particle size by excess lead was studied in the second stage. After the amorphous and agglomeration were reduced to acceptable region. The optimal objective of the research is to develop a semi-continuous process which may be applied in manufacturing PZT nanoparticles with small sample variations. The final stage, production rate and cost effectiveness are studied by adjustments with the finding on the first two stages. Small adjustments such as mineraliser concentration and percentage excess lead used in the

system are used to optimize the quality of the PZT nanoparticles with the semi-continuous process.

Chapter 2
Control particle size and morphology via controlling ramping & cooling

2.1 Introduction

Using the ramping and cooling rates to control size and distribution of PZT nanoparticles is theoretically sound. As shown in Figure 4, there is no nucleation before the concentration reaches the minimum requirement saturation level (cf. Region I) [10]. Once nucleation starts, growth starts as well (cf. Region II of Figure 4). When the concentration falls below a critical concentration, nucleation stops but growth continues (cf. Region III of Figure 4). By increasing the ramping rate, a super-saturation state is quickly achieved resulting in a very narrow region II, illustrated in Figure 4. Higher ramping rate means higher initial supersaturation and larger number of

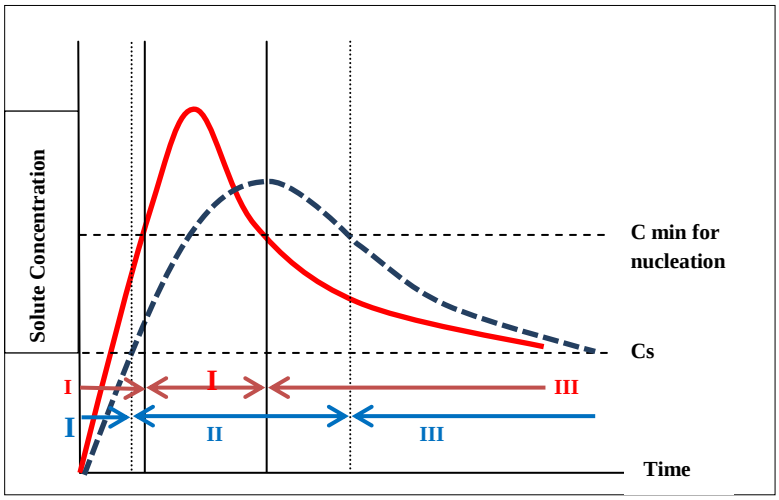

Figure 4 Illustration of the process of nucleation and subsequent growth where region II is nucleation zone and region III is growth zone (Dash line: lower ramping; Solid line: higher ramping rate)

nucleation sites. This promotes formation of larger number yet smaller size of nuclei for a given solute concentration. Moreover, higher initial supersaturation means higher nucleation rate, as illustrated in Figure 4. Therefore, nucleation will be dominated over growth in region II [10]. As a result, all nucleation would occur at the same time (high nucleation density) but with very limit time for growth, which subsequently leads to a smaller particle size and narrow size distribution.

By increasing the cooling rate, the concentration can be brought to a thermodynamic equilibrium very quickly to stop the crystal growth thus controlling the final particle size and morphology. Soon after the primary stage of the growth (region III in Figure 4), Ostwald ripening occurs, leading to the secondary stage of nucleation and growth. In the secondary stage, aggregation process dominates leading to agglomeration and coagulation of the particles [19]. For hydrothermal processes, crystal growth highly depends on convective mass transfer of the dissolved part of the substance [20]. Increasing the cooling rate can significantly slow down the convective mass transfer and shorten the secondary stage, thus controlling the final particle size and improve the morphology effectively.

2.2 Experimental procedure

2.2.1 General PZT feedstock preparation

The experimental procedure is a modification of the synthesis procedure developed by Su et al[1]. As a first step, tetra-iso-propyltitanate, $Ti(OCH(CH_3)_2)_4$ [denoted as TIPT] was mixed with acetylacetone [denoted as AcAc]. The mixture was continuously stirred under room

[1] B. Su, T. W. Button, C. B. Ponton, "Control of the particle size and morphology of hydrothermally synthesized PZT powder," *Journal of Materials Science*, 2004, Vol. 39, pp. 6439-6447,

temperature for 4 hours, and Zirconium acetate, $Zr[O(CH_2)_2CH_3]_4$ was added after stirring. Next, the mixture of Ti and Zr sources was dropped into a 1-M potassium hydroxide (KOH) solution. White precipitation $(Ti/Zr)O_2$ was formed during this process. Centrifuge was used to separate the white precipitation from the residual KOH solution. The precipitation was washed with DI water till it was pH neutral. The white precipitation (in the form of gel) was then mixed with Lead acetate trihydrate, $Pb(C_2H_3O_2)_2$, powder. Next, the mixture was added into a second KOH solution (serving as a mineraliser), whose concentration can be varied to control size and morphology of resulting PZT nanoparticles. Same general PZT feedstock preparation is used for all trials but different chemical molar ratio, concentration of the mineraliser, and various hydrothermal processes may be applied.

2.2.2 Hydrothermal process

After all the chemicals were well mixed in the mineraliser, it was sealed in an autoclave and went through a hydrothermal growth in a furnace. During the hydrothermal process, various combinations of ramping rate, processing time and cooling time are tried to obtain suspension with PZT nanoparticles. The suspension product from hydrothermal was centrifuged, washed with DI water till pH was neutral, and then the PZT particles were oven-dried under 80˚C for evaluation, such as SEM or XRD.

During the stage of the research, the experiments were repeated with some parameters always being fixed, while others varied from trial to trial. The fixed parameters include (a) molar ratio of each chemical (except the mineraliser) and (b) the amount of the PZT precursor injected in the autoclave and the furnace during the hydrothermal growth.

2.2.3 Parameters

The following parameters are varied during the trials. First, the mineraliser concentration used included 2M and 5M. Second, ramping rate was chosen to be 5^0C/min, 10^0C/min, and 20^0C/min. Third, hydrothermal processing time was controlled in 1 hour ~ 5 hours, depended on mineraliser concentration. Finally, three cooling rates are employed: slow (~1.5˚C/min), medium (~2.8˚C/min), fast (~3.6˚C/min), and very fast (~5˚C/min). For the slow cooling rate, the autoclave is cooled down in the furnace with the furnace door closed. For the medium cooling rate, the autoclave was first kept in the closed furnace for some time and the furnace door was later opened to expedite the cooling. For the fast cooling rate, the furnace door was opened right after the hydrothermal process is completed with the autoclave stayed inside of the furnace. For the very fast cooling rate, the autoclave was removed from furnace immediately after the hydrothermal process is completed.

In studying the effects of ramping rates, two benchmark hydrothermal syntheses are used. One uses mineraliser concentration of 2M, processing time of 3 hours, and very fast cooling rate (~5˚C/min). The other uses mineraliser concentration of 5M, processing time of 1 hours, and very fast cooling rate (~5˚C/min). Moreover, test results are labeled using following notation A-B-C-D, where A is the processing time in hour, B is the ramping rate in ºC/min, C is the mineralizer concentration in M (mol/L), and D is the cooling rate (e.g., “vf” for very fast cooling rate).

2.3 Experimental Result

X-ray diffractometry (XRD) measurements and Scanning electron microscopy (SEM) of PZT nanoparticles produced under the benchmark condition with three ramping rates and cooling rate are shown in Figure 5-9. The XRD patterns are compared with a PZT database using JADE 7.0 to confirm the resulting product is indeed PZT, and all major peaks are labeled. SEM images are used to observe morphology and particle size of resulting PZT nanoparticles. Noted that 10M samples are not discussed here since there is no PZT nanoparticles were successfully fabricated, regardless of the choice of ramping or cooling rate.

2.3.1 Effects on processing time

Based on our theory, longer processing time means longer growth time and larger particle size. Also, it is known that processing time and mineraliser concentration influent the particle size. Therefore, it is important to find the correlation between the necessary processing duration with a certain chosen mineraliser concentration.

For example, from Figure 5, with 2M mineraliser concentration, 2 hour processing time is not enough to form PZT the proper morphology even though it was identified as PZT through XRD. Samples with 5 hour processing time

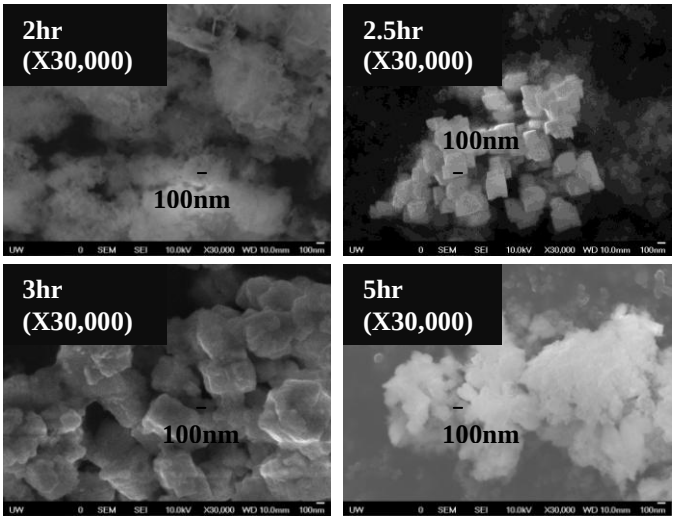

Figure 5 Illustration on relationship between processing time and mineraliser concentration

show severe agglomeration. Both these cases have PZT particles that have little practical usage. Increasing the processing time to 2.5 hour, the resulting PZT particles have much better morphology and 3 hour sample shows great morphology. The similar trial was applied on 5M mineraliser concentration samples with slow cooling rate (~1.5˚C/min). For 5M samples, the formation of PZT requires as short as 1 hour, shown in **Error! Reference source ot found.**. However, the degree of agglomeration was too severe for observation in changes in morphology and particle size. The sample with 20˚C/min ramping rate demonstrates the severe agglomeration in Figure 6. Therefore, 2M mineraliser, 3 hour processing time, and very fast cooling rate (~5˚C/min) is used to observe the effects on ramping rates.

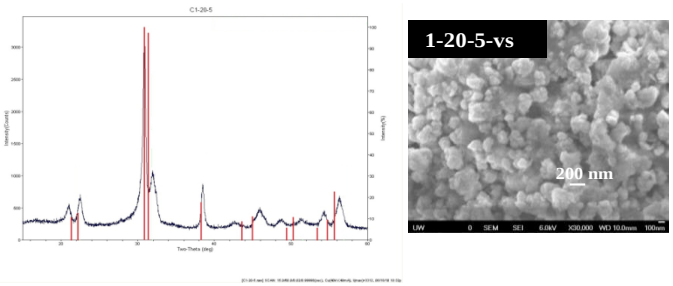

Figure 6 XRD pattern (left) and SEM image (right) of ramping trials for benchmark mineraliser concentration (5M), processing time (1 hour), and very slow cooling rate

2.3.2 Effects on Ramping rates

2M mineraliser concentration and 3 hours hydrothermal growth with very fast cooling rate (~5˚C/min) is used to illustrate the effects on ramping rate. XRD patterns, Figure 7, show PZT composition and have the same peak locations (which means that overall similar crystal structure), the high ramping rate

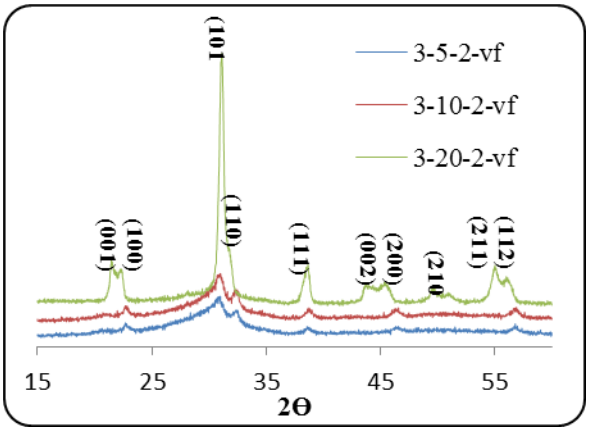

Figure 7 XRD pattern of ramping trials for benchmark mineraliser concentration (2M), processing time (3 hours), and very fast cooling rate

(20˚C/min) sample shows relatively small intensity in the secondary phases while the lower ramping rate samples (5˚C/min and 10˚C/min) contain readily secondary phase. For example, lower ramping rate samples (5˚C/min and 10˚C/min) contain obvious $PbTiO_3$ phase (around 2Θ ~ 32˚). At lower 2Θ region, split peaks of (001) and (100) is observed indicating the presence of both rhombohedral ($PbZrO_3$) and tetragonal ($PbTiO_3$) phases [21]. These two peaks both have higher intensity than the database. It may be contributed by different composition of $Pb(Zr_x,Ti_{x-1})O_3$, such as $Pb(Zr_{0.8}Ti_{0.2})O_3$. All of them have board peaks at (002) and (200) which are contributed by $PbTiO_3$ formation. The broadened peak may be contributed by $PbZrO_3$ phase [14]. In addition, the intensity and sharpness of the XRD shown in the high ramping rate sample indicates increasing in crystallinity [13], which is an evidence of better PZT quality.

Figure 8 shows SEM images (magnification 10,000X) of the three samples with ramping rate 5˚C/min, 10˚C/min and 20˚C/min. The sample with the 5˚C/min ramping rate presents large aggregates and severe agglomeration. The sample with the 10˚C/min ramping rate shows large aggregates, and the sample with the 20˚C/min ramping rate has smaller aggregates. Although a higher ramping rate could reduce aggregation, it cannot completely eliminate the aggregation. Aggregation needs to be removed via other methods in order for these PZT nanoparticles to be useful.

Figure 8 also shows SEM images (magnification 30,000X) of PZT nanoparticles produced under the two ramping rates: 10˚C/min and 20˚C/min. (The SEM 30,000X image for the sample with the 5˚C/min ramping rate could not be obtained due to the severe agglomeration.) As shown in Figure 8, PZT sample produced under the ramping rate of 10˚C/min consists of very fine particles with size around 100 nm and their morphology is more spherical. In contrast, PZT

nanoparticles produced under the ramping rate of 20˚C/min has particle size ranging from 200 nm to 600 nm. Also, morphology of the PZT nanoparticles is clearly cubic. This indicates that the high ramping rate has a significant effect on the morphology.

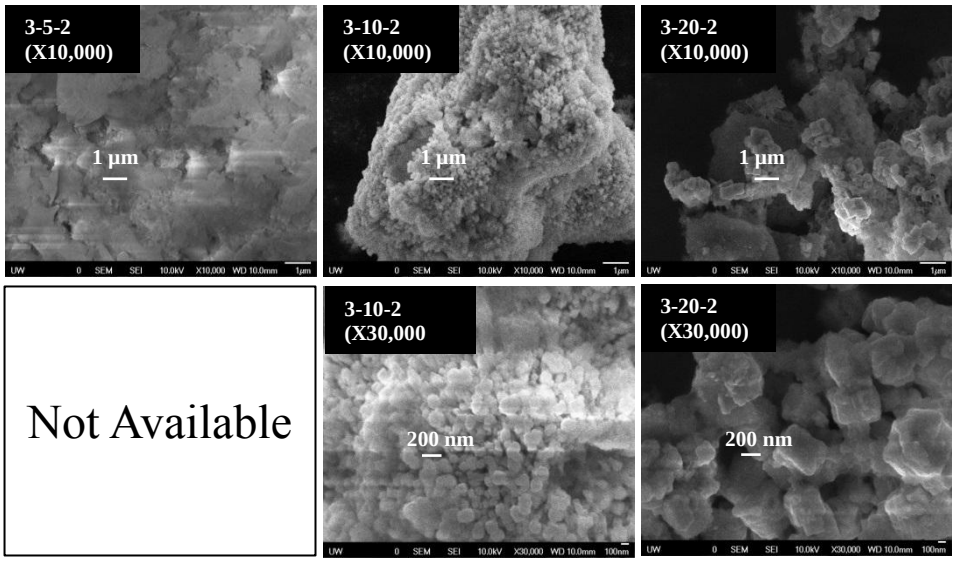

Figure 8 Samples with 3M KOH, 2-hr growth, and very fast cooling rate with ramping 5˚C/min (left), 10˚C/min (center) or 20˚C/min (right)

Controlling growth of PZT nanoparticles via hydrothermal synthesis is indeed a fairly complex task, because multiple process parameters are involved. In Figure 8, we see a dramatic effect of the ramping rate given the benchmark parameters above. The effect of the ramping rate, however, may not be as dramatic under other process parameters (e.g., if a very slow cooling rate of 1.5˚C/min is used). Therefore, using high ramping rate is favorable in achieving the desirable cubic morphology and particle size while reducing aggregation at the same time.

2.3.3 Effects on Cooling Rates

In studying the effects of cooling rates, we use a benchmark hydrothermal synthesis as follows: mineraliser concentration of 5M, processing time of 1 hour, and high ramping rate (20˚C/min). Four cooling rates are used as defined earlier. The same notation A-B-C-D is used to denote these four process parameters.

Figure 9 shows the XRD of the samples under the four cooling rates. From Figure 9, peak locations do not change much with respect to the cooling rates. This implies that the cooling rates do not affect the chemical composition significantly. Nevertheless, secondary phases such as $PbTiO_3$ appear when the cooling rate is lower. For example, for the medium cooling rate (2.8 ˚C/min), secondary phases of $PbTiO_3$ are found (100) at the low-angle range, (110) and (002) at the mid-angle range, and (211) in the high-angle range. This shows that $PbTiO_3$ dominates when cooling rate is slow. This occurs because lower energy is needed in forming a tetragonal structure (e.g., $PbTiO_3$) [14]. Note that the sample with very slow cooling rate (1.5˚C/min) has poor crystallinity and result in lower peak intensity for all major peaks.

For the case of fast and very fast cooling rates, secondary phases are more difficult to identify because many peaks that correspond to the PbTiO3 tetragonal phases overlap or merged with $PbZrO_3$ rhombohedral phases Figure 9. Nevertheless, the high intensity (110) peak

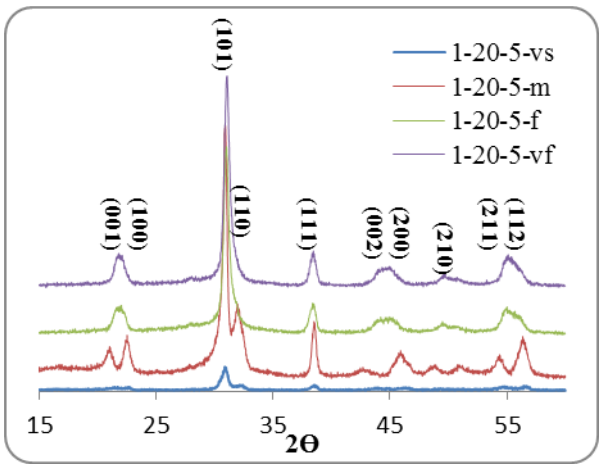

Figure 9 XRD pattern for samples with various cooling rate (5M KOH with 1 hour processing time with ~1.5˚C/min (vs), ~ 2.8˚C/min (m), ~3.6˚C/min (f), and ~5˚C/min (vf) cooling rate

of $PbTiO_3$ is not present, implying that there is no or low secondary phases.

Figure 10 shows SEM images (magnification 30,000X) of the PZT nanoparticles under the four cooling rates. The sample with very slow cooling rate (~1.5˚C/min) has severe agglomeration. Therefore, the particle size cannot be determined by the SEM image. The sample with the medium cooling rate (~2.8˚C/min) results in high degree of agglomeration but the morphology is significantly improved as the cubic structure starts to appear. The medium cooling rate results in particle size in 600 nm to 800 nm range. The sample with the fast cooling rate (~3.6˚C/min) has particle size from 200 nm to 600 nm. Some samples show aggregates that are chemically bonded thus increasing overall particle size. As the cooling rate increases further, the overall particle size decreases to a range of 200 nm to 400 nm for very fast cooling rate (~5˚C/min). In conclusion, the SEM images in Figure 10 show that the cooling rate is an effective way to control the size of PZT nanoparticles.

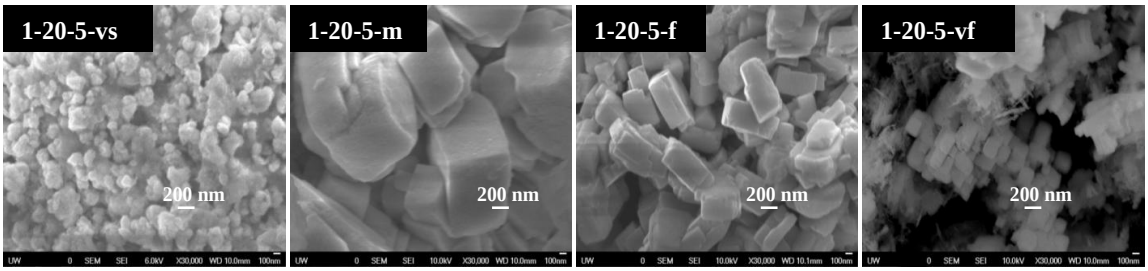

Figure 10 Samples with 5M KOH and 1 hour processing time with various cooling rate (slowest (~1.5˚C/min) to fastest (~5˚C/min) from left to right)

2.4 Summary and Conclusions

Using nucleation and subsequent growth theory to control morphology and particle size is proved to be a sufficient method. With two chosen mineraliser concentration-- 2M and 5M, processing times to ensure the formation of PZT are 3 hours and 1 hour, respectively. After the proper hydrothermal growth times are determined, effects on ramping rates and cooling rates were studied to verify the theory. Stop growth, equivalent to high cooling rate, seems to have stronger influence on particle morphology. Based on the study on effects on the ramping rates with 5M mineraliser concentration, observations in morphology and particle size were difficult in all slow cooling samples, regardless of the choice of cooling rates. In addition, combining the highest ramping rate (20˚C/min) and the highest cooling rate (~5˚C/min), quality of the PZT nanoparticles is improved significantly, regardless of the choice of mineraliser concentrations. The resulting particle size is in the range of 200 nm to 800 nm under these two combinations, which is within the required particle size range. These two trials also suggested that lower mineraliser concentration in the system will require longer time for PZT completely formed. It could mean that mineraliser also promote nucleation to occur in a short period of time and create high nucleation density. However, using mineraliser concentration to control the process is more troublesome since the processing time will also need to change as well.

Chapter 3
Modification by excess lead

3.1 Introduction

Although we have successfully demonstrated that control of ramping and cooling rates is an effective way to control the size of PZT nanoparticles in the range of 200 nm to 600 nm with cubic crystal morphology, there are two remaining problems. One is agglomeration and aggregation of the PZT nanoparticles. The other is presence of amorphous phase in the PZT nanoparticles. Use of excess lead could significantly alleviate both problems. It is very common that lead deficiency, which is a cause of the problems, occurs in the beginning of the hydrothermal process. Therefore, supply of excess lead can effectively compensate the lead deficiency [15, 17].

For example, Gersten [19] shows that agglomeration can be significantly reduced, if the mineraliser concentration (KOH) is between 2M and 4M and the lead concentration is between 0.5M and 0.6M. Traianidis [15] uses excess lead to reduce amorphous phase. The lead deficiency causes the Pb/(Ti, Zr) molar ratio to fall below 1, which is required for PZT formation, thus lowering ion activities. Excess lead can ensure the required Pb/(Ti,Zr) molar ratio and high ion activities, resulting in improved crystallinity and reduced amorphous phase [15].

3.2 Experimental procedure

Based on Gersten's finding, we use the following benchmark parameters to study removal of the aggregation and amorphous state. The mineraliser concentration is 2M, the processing time is 3 hour, the ramping rate is (20˚C/min), and the cooling rate is very fast (~5˚C/min). Moreover, samples with 5 different lead concentrations are prepared: 0.38M (0% wt. lead excess), 0.41M (10% wt. lead excess), 0.45M (20% wt. lead excess), 0.53M (40% wt. lead excess), and 0.68M (80% wt. lead excess). Rest of the PZT feedstock preparation and molar ratio on raw materials remind the same. Introducing excess lead into the system means that there could be residual unreacted lead or lead byproducts which are considered impurities if reminding in the system. Therefore, an additional post process step of washing the resulting suspension from hydrothermal growth is applied. Diluted 10% vol. acetic acid is used to wash the suspension after it is washed with DI water. Then, after the solution layer is clear after centrifuge, the suspension is washed with DI water again to bring pH back to neutral.

3.3 Experimental Results—modification

Figure 11 shows XRD measurements from samples processed under the condition of 2M KOH and 3-hour processing time. Five samples with excess lead of 0%, 10% wt., 20% wt., 40% wt., and 80% wt. are measured. The XRD measurements are very consistent, indicating that the presence of excess lead does not affect crystal structures (e.g., shape and lattice parameters). The

width at half maximum has little variation from sample to sample. This implies that crystal size of the PZT nanoparticles does not change significantly[2].

Figure 13-14 show SEM photos of samples with 0% wt. to 80% wt. of excess lead. Figure 13 has magnification of 1000 focusing on the overall amorphous region and agglomeration reduction. Figure 12 has magnification of 10,000 revealing reduction of agglomeration as the amount of excess lead increases. Figure 14 has magnification of 30,000 demonstrating the particle size and morphology.

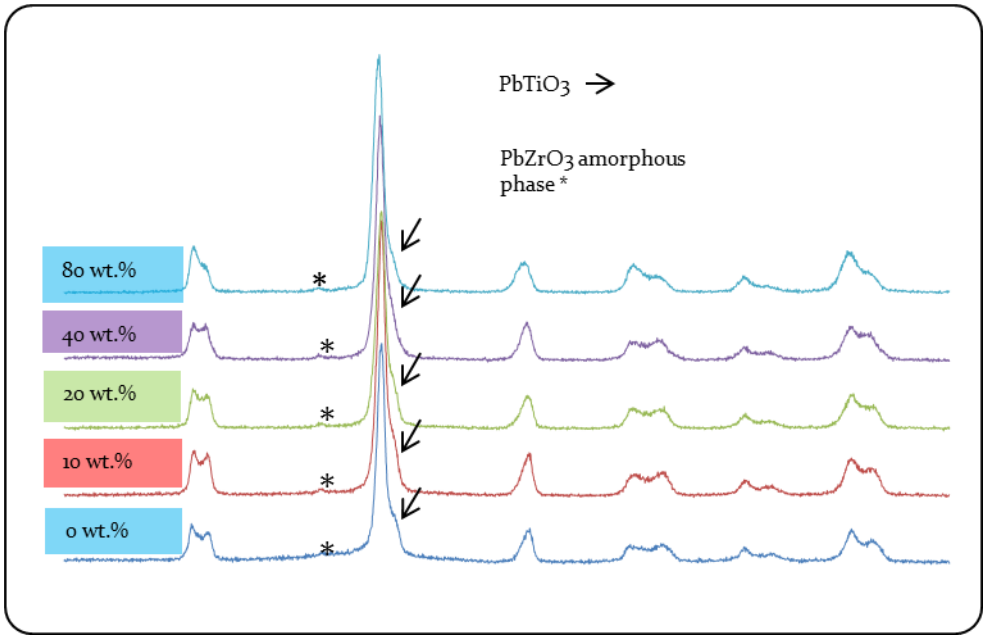

Figure 11 XRD patterns for lead concentration trial (2M KOH and 3 hour processing time)

[2] Please note that crystal size is different from particle size. Crystal size is a quantity from the smallest repeatable structure, while particle size is measured from scanning electron microscopy (SEM).

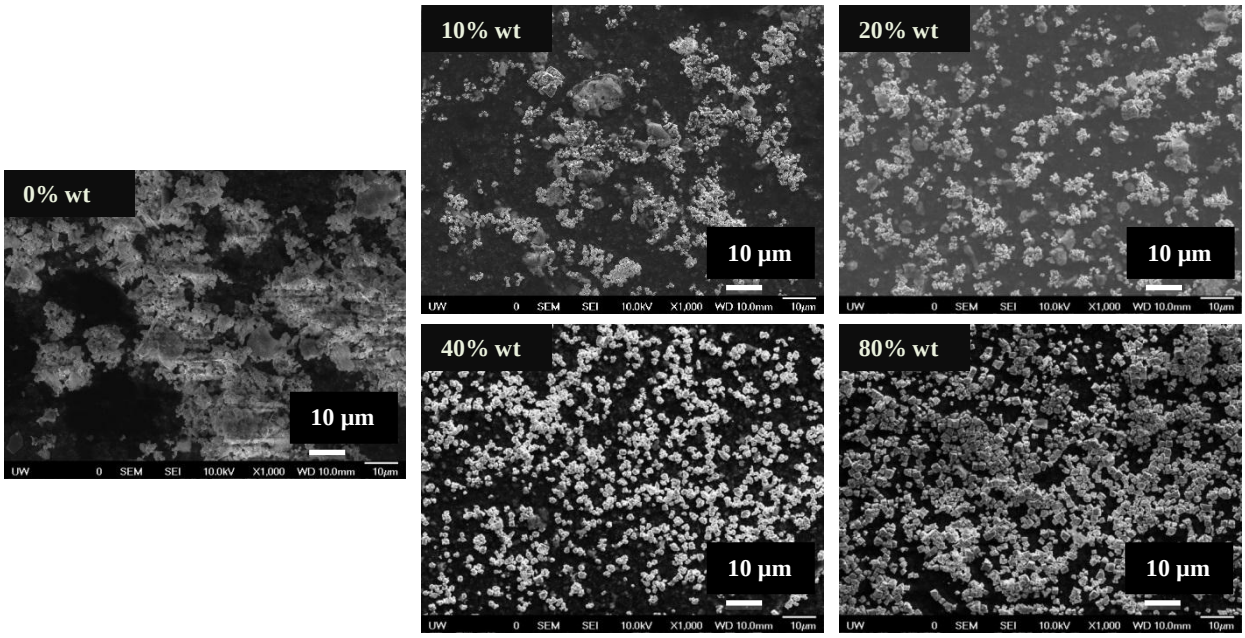

Figure 13 SEM images on excess Pb samples (X1,000) with 2M KOH and 3 hour processing time

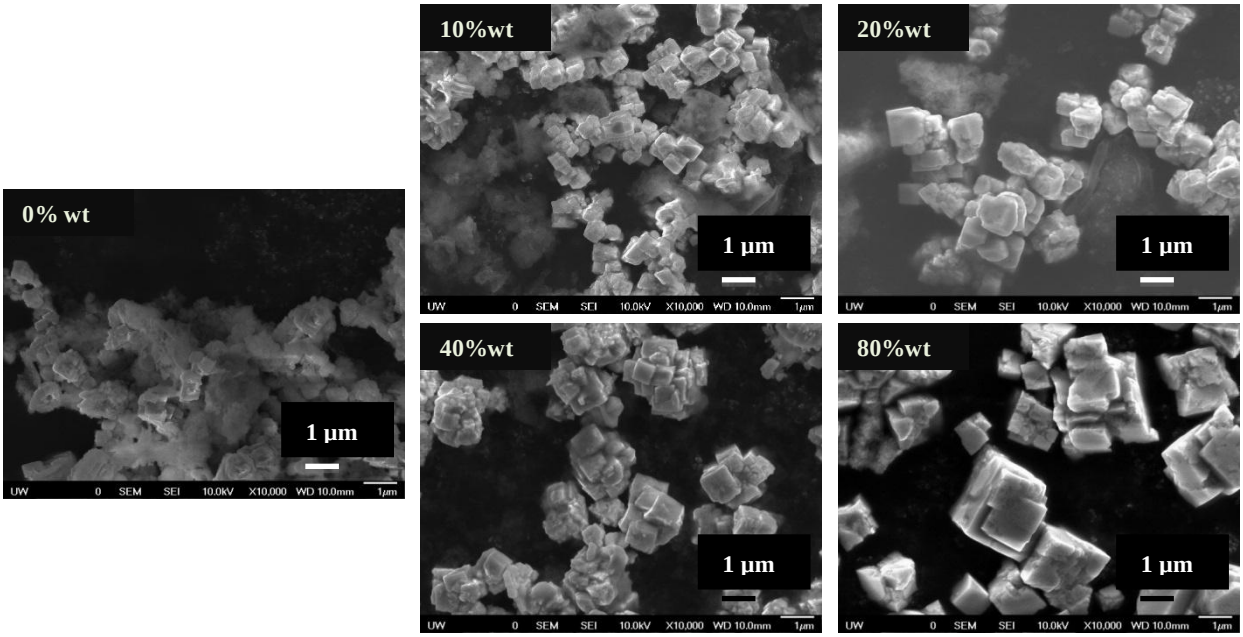

Figure 12 SEM images for excess Pb (X10,000) (2 M KOH and 3 hour processing time)

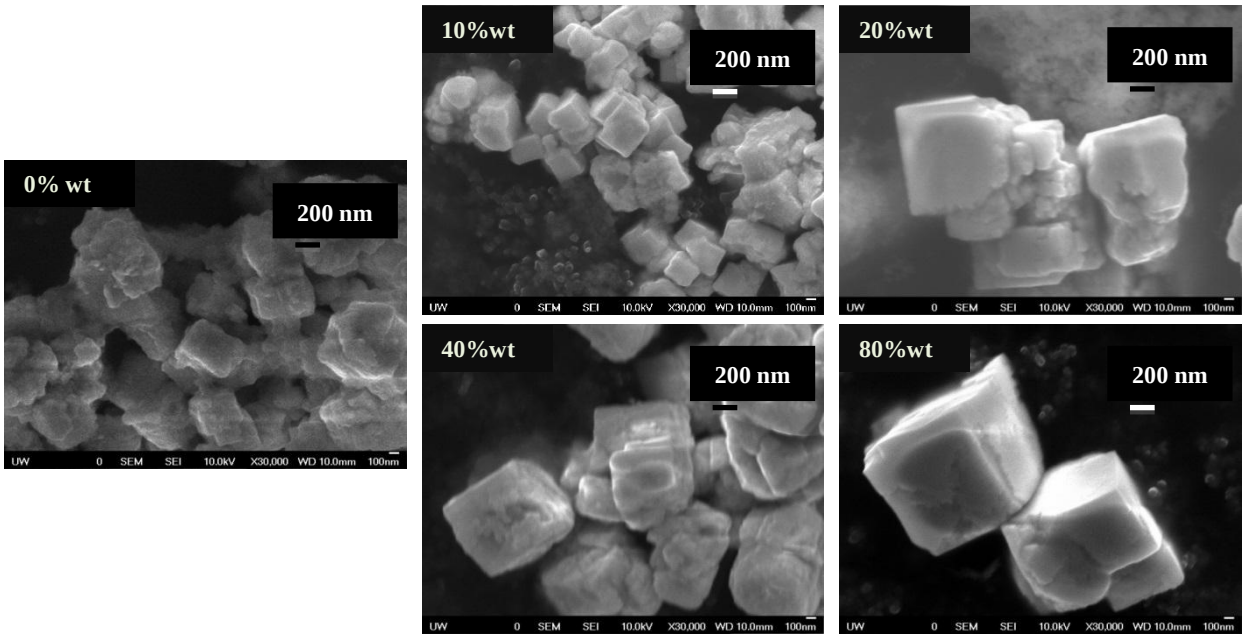

Figure 14 SEM images for the excess Pb samples (X30,000) (2M KOH and 3 hour processing time)

From Figure 13-14, reduction of amorphous phase is obvious as excess lead increases from 0% wt. to 80% wt. Even a little excess lead (e.g., 10% wt.) shows a huge reduction of amorphous region. The excess lead also reduces agglomeration. From Figure 12 and 13, the degree of agglomeration is inversely proportional to the amount of excess lead used. For the 80% wt. sample, the PZT particles are almost free of agglomeration.

The excess lead, however, increases the particle size; see Figure 14. Nevertheless, the particle size remains within the allowable range (200 nm- 800 nm). After all, it is better to have larger particles with less agglomeration than otherwise.

3.4 Summary and Conclusions

Table 1 Summary of effects on various lead concentrations summarized the result from excess lead trial. By introducing excess lead into the system, amorphous phase was successfully removed and degree of agglomeration was reduced significantly. However, the downside is that the particle size increases as percentage weight of excess lead increases. Therefore, it is necessary to find a balance between aggregate sizes resulted from agglomeration and particle size.

Table 1 Summary of effects on various lead concentrations

Excess Lead (%wt)	Particle Size (nm)	Aggregate Size (μm)	Observation
0%	300±100	>10	▪ Few particles around 1 μm ▪ High degree agglomeration ▪ Large amount of amorphous
10%	300±100	1-10	▪ Few particles around 1 μm ▪ High degree agglomeration ▪ Some amorphous
20%	400±100	1-6	▪ Few particles around 10 μm ▪ Lower degree of agglomeration ▪ Little amorphous
40%	650±200	1-2	▪ Most particles agglomerate into 1 μm size aggregates ▪ Low degree agglomeration ▪ No amorphous
80%	800±200	1-2	▪ Particles and aggregates are around 1μm ▪ Very low degree agglomeration ▪ No amorphous

Chapter 4
Development of Semi-Continuous process and Quality control

4.1Introduction

From chapter 3, the recipe we have developed thus far uses 80% wt. excess lead and 2M of KOH mineraliser concentration. The hydrothermal process includes high ramping rate 20˚C/min, process temperature 200˚C, process time of 3 hours, and very fast cooling rate (~5˚C/min). This recipe reduces the presence of amorphous phases and the degree of agglomeration while maintaining desirable cubic morphology and correct chemical composition. For the rest of the paper, a process with these parameters is called an "optimal non-continuous process" (ONCP).

The ONCP, however, has a major drawback—the overall time for the production of PZT nanoparticles is very long. The bottleneck is the ramp-up of the furnace from the room temperature, because cooling of the furnace to the room temperature from a prior batch takes a

long time (roughly 2 to 3 hours). Also, 80% wt excess lead would increase manufacturing costs due to excess material and waste handling. Therefore, a continuous process is developed to reduce the overall process time while minimizing the excess lead contents. The detail procedure is described as follows.

First, no ramping is involved, and the furnace is maintained at 200˚C all the time. Second, the feedstock contains 2.5M KOH mineraliser as well as 50% wt. excess lead. Third, the autoclave with the feedstock is placed directly in the furnace and goes through hydrothermal growth for 2 hours. Then the autoclave is removed from the furnace to cool down in the air under the room temperature. The process is repeated till the feedstock is used up and the process is called "Semi-continuous process" (SCP).

4.2 Finalized synthesis procedure

4.2.1 PZT feedstock preparation

The general PZT feed stock preparation procedure from Ch.2 still applies. The amount of lead acetate trihydrate is 50% wt. more than its requirement since 80% wt. excess lead will lead to samples with larger particles and resulting in higher material waste. Next, the mixture is added into a second KOH solution (serving as a mineraliser) with a concentration of in range of 2.5M to 3.5M from 2M, as stated in Ch.3, in order to shorten the required hydrothermal growth time. The purpose of the modification in this stage is to balance in cost of fabrication and material quality (which will explain in more details in later section).

4.2.2 Finalized hydrothermal process

The hydrothermal process was modified to scale up the production as follows. First of all, the oven is kept at the hydrothermal processing temperature (200˚C) constantly to eliminate time needed for furnace to ramp and to cool. After all the chemicals were well mixed in the mineraliser, it was sealed in an autoclave (containing 10 ml of PZT precursor) at the room temperature. The autoclave is then placed in the oven directly. After 2 hours of hydrothermal growth, the autoclave is taken out of the oven and cooled in the room temperature to obtain suspension with PZT nanoparticles. (Note that the hydrothermal growth time is reduced as a result of increased concentration of the mineraliser.) Since the modified process no longer requires ramping and cooling of the furnace, it saves 3 hours in processing each autoclave, and the production rate is almost tripled.

The suspension from the autoclave was centrifuged, washed with 10% vol. diluted acetic acid to remove un-react lead, and washed with DI water till pH was neutral, and then the PZT particles were oven-dried for evaluation, such as SEM or XRD.

4.3 Quality Control

In order to check if the semi-continuous process is stable and can produce PZT nanoparticles with acceptable range, monitoring the quality of the nanoparticles are important. As before, XRD is used to identify if the nanoparticles are indeed PZT and SEM is used to observe the amorphous phase, degree of agglomeration, and particle size. Figure 15 shows XRD patterns with the sample from ONCP and SCP. The top black pattern is the sample with ONCP

(i.e., 80% wt. excess lead) as a baseline, and the rest is from the samples with the SCP. There are several issues worth noting. First, peaks from all samples appear at the same location. This implies that all samples have similar lattice parameter. Second, relative ratios of peak intensity are similar for all samples. This implies that crystal structures and crystallinity are similar for all samples. Note that peak intensity itself does not play a key role, because many other factors than crystal structures can affect the peak intensity. In contrast, relative intensity is a better way to identify variations among samples.

Figure 16 (magnification 5,000X) compares the results from ONCP and SCP samples. The aggregates in the SCP sample are slightly larger but all around 1 μm with little agglomeration. Also, the SCP sample shows no amorphous regions. These images demonstrate that ramping removal does not significantly affect the degree of agglomeration, aggregate size, and particle size. This is consistent with the observation that excess lead with greater than 40% wt. will completely remove the amorphous state [19].

Figure 16 (magnification 30,000X) shows SCP samples from different batches. Note that different batches may have some variations in mineraliser concentration due to difficulty in controlling precise weight of KOH (mineraliser) pellets. We estimate that the mineraliser concentration could at most vary between 2.5M and 3.5M from batch to batch. Nonetheless, all samples show low degree of agglomeration, 1-2 μm in aggregate size, and 300-600 nm in particle size. All the SCP samples do not contain amorphous regions and have good morphology. The SCP samples are quite uniform and are not sensitive to the change in mineraliser concentration. All evidence indicates that SCP is a very stable and reliable process.

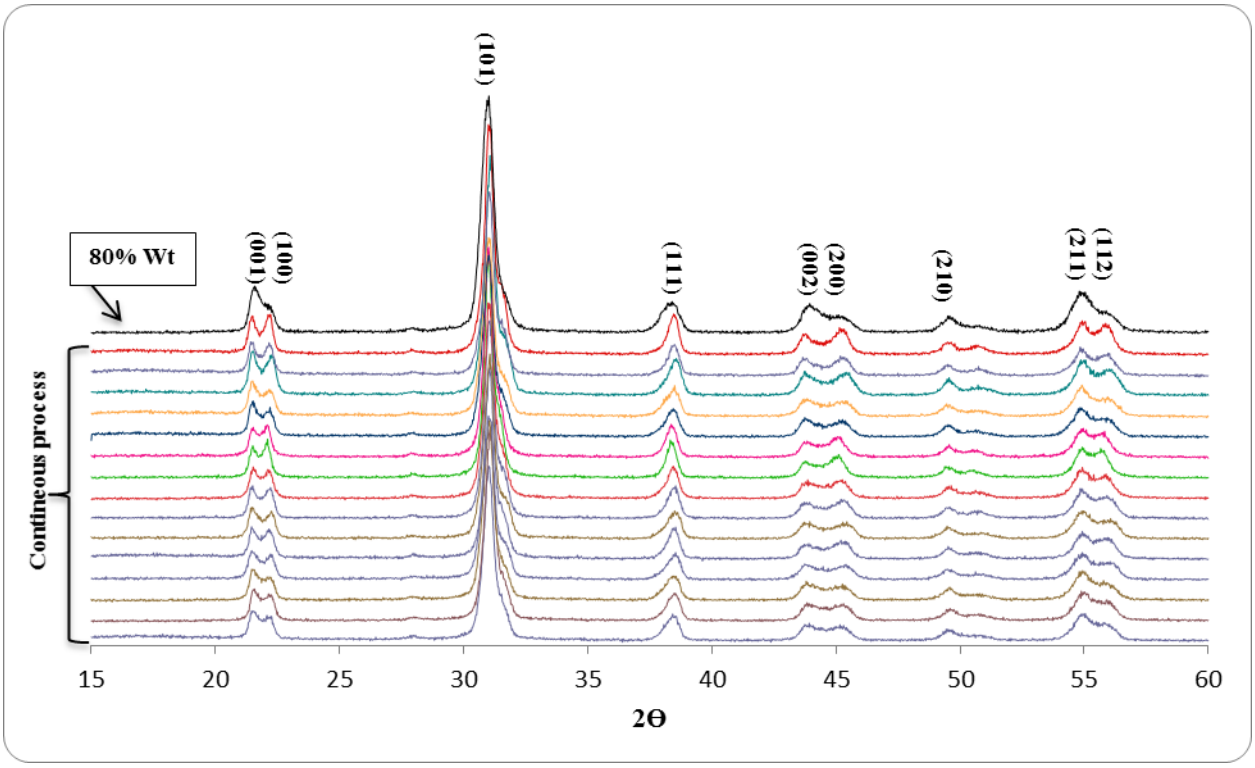

Figure 15 Measured XRD patterns for 80% wt. excess lead sample and continuous process samples (All samples are from different batch of PZT feedstock)

Figure 16 (magnification 5,000X) compares the results from ONCP and SCP samples. The aggregates in the SCP sample are slightly larger but all around 1 μm with little agglomeration. Also, the SCP sample shows no amorphous regions. These images demonstrate that ramping removal does not significantly affect the degree of agglomeration, aggregate size, and particle size. This is consistent with the observation that excess lead with greater than 40% wt. will completely remove the amorphous state [19].

Figure 17 (magnification 30,000X) shows SCP samples from different batches. Note that different batches may have some variations in mineraliser concentration due to difficulty in controlling precise weight of KOH (mineraliser) pellets. We estimate that the mineraliser concentration could at most vary between 2.5M and 3.5M from batch to batch. Nonetheless, all samples show low degree of agglomeration, 1-2 μm in aggregate size, and 300-600 nm in particle size. All the SCP samples do not contain amorphous regions and have good morphology. The SCP samples are quite uniform and are not sensitive to the change in mineraliser concentration. All evidence indicates that SCP is a very stable and reliable process.

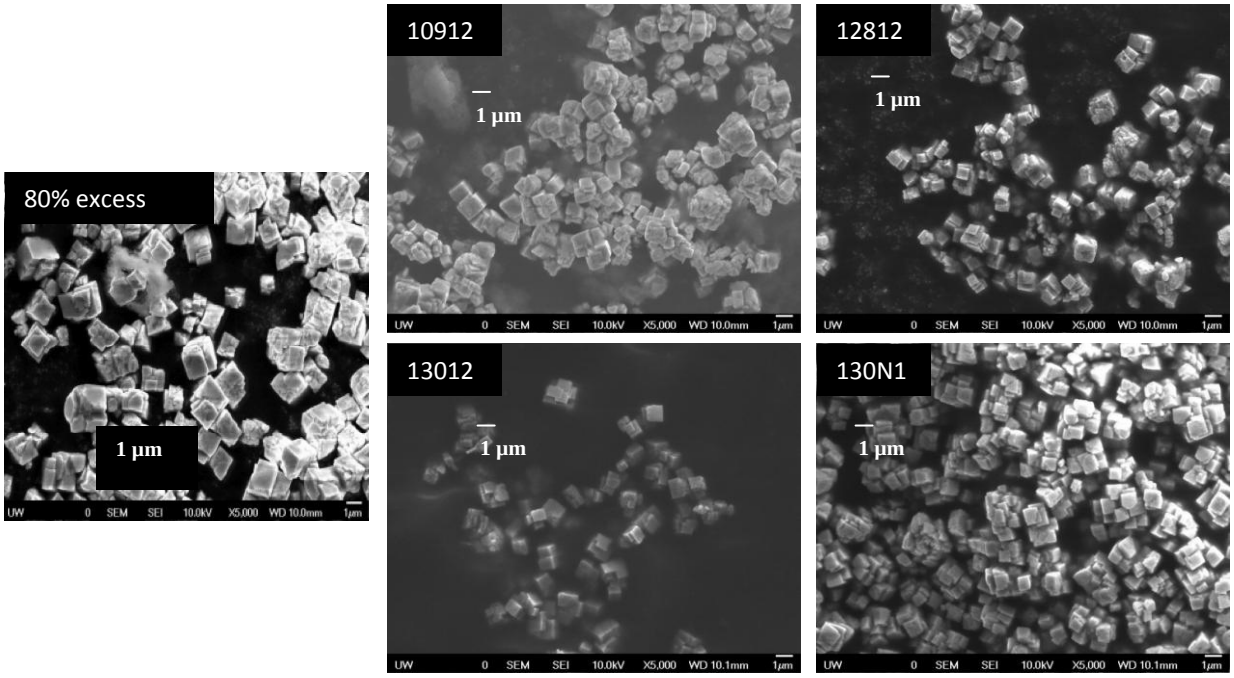

Figure 16 Left: 80% Pb excess sample; Right: Semi-continuous process sample (5,000X)

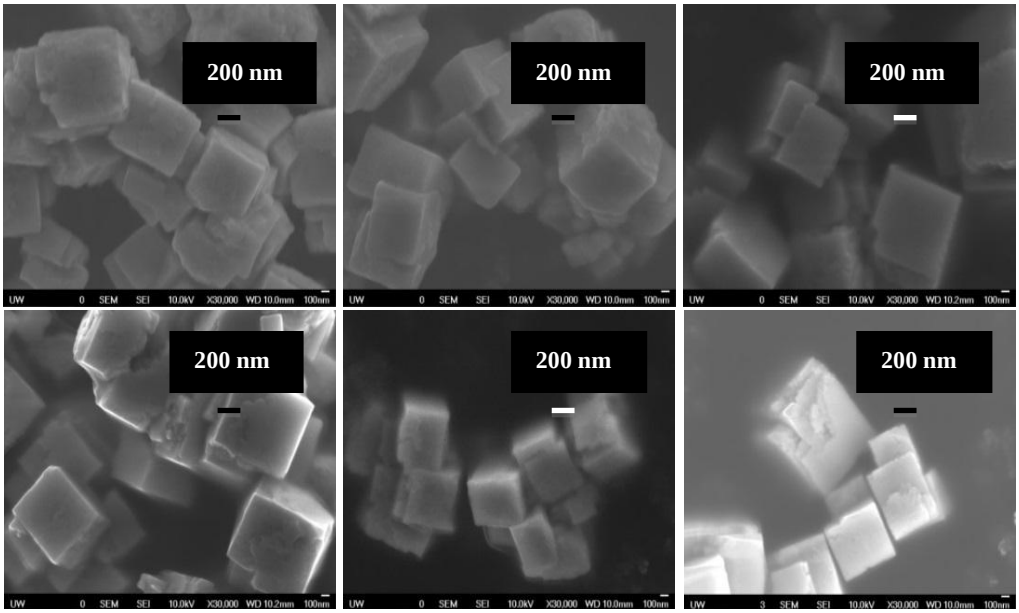

Figure 17 SEM image of Semi-continuous process (X30, 000)

4.4 Estimation on production effectiveness

After the quality of the PZT nanoparticles fabricated via SCP was confirmed, we now can compare the effectiveness in between ONCP and SCP, which is summarized in Table 2. The production rate every 8 hours is almost tripled. Increasing in production rate is highly desirable for manufacturing purpose since it can lower the cost of raw material (PZT) for sensor fabrication or other purpose. It is also important in research project that joins forces with industry since industry generally requires a certain amount of printing medium in order to run their printing system. For example, a 20% solid content PZT ink requires about 10g PZT nanoparticles which will take around 80 hours for ONCP but only around 24 hours for SCP. Notice that here, raw material cost is not considered since raw materials are not expansive. Therefore, reducing excess lead from 80% wt. to 50% wt. does not save much on cost of the raw material. However,

the cost of reduction in hazardous material handling is significant since lead is considered as a hazardous material and requires professional handling on disposal.

Table 2 Production comparisons between ONCP and SCP

	ONCP	**SCP**
Ramping time (min)	10	N/A
Hydrothermal growth (min)	180	120
Cooling time (min)	120-180	N/A
Yield each cycle (g)	0.7-0.8	0.7-0.8
Production rate (per 8 hours)	~1.1	~3.2

4.5 Summary and Conclusions

During the optimization stage, the semi-continuous process is developed with some adjustments in hydrothermal growth based on the best sample from Ch.3 (80% wt. excess lead sample). Mineralisr concentration changed from 2M to 2.5 M ~ 3.5 M. Excess lead reduced from 80% wt. to 50% wt. Processing time reduced from 3 hours to 2 hours. Ramping and cooling rate are removed. It means that one un-processed autoclave was swapped with one processed autoclave every 2 hours. The resulting PZT nanoparticles appear to have very small sample variations in terms of crystal structure (microstructure), morphology, and particle size. XRD patterns show that all samples have almost identical crystal structure. SEM images verify that resulting PZT nanoparticles still remind to have no amorphous region and very low degree of agglomeration even with slightly higher mineraliser concentration and slightly lower excess lead

compared to the best scenario from Ch.3. Therefore, we can conclude that the SCP can be further developed into manufacturing process with using the same concepts.

Chapter 5
Future works

5.1 Overview

Now that SCP is verified as a stable and reliable process, characterization of material properties, PZT ink fabrication, sensor fabrication, and performance measurements can begin. All these will require large quantity of PZT nanoparticles. The quality of the PZT nanoparticles should be continuously observed. However, examination of every single sample is probably not necessary since samples from the same batch use the exact same feedstock and sample variations are expected to be small. Therefore, one random sampling from each batch should be sufficient enough.

5.2 Characterization of material properties

Characterization of material properties including chemical composition, mechanical properties, and electrical properties should be determined. The purpose of characterization of material properties is to have a more in depth understanding on the PZT nanoparticles and prepared for the next step—ink fabrication and sensor fabrication. Since PZT nanoparticle

fabrication is done in the house, there are no known properties, which make it very difficult to make predictions on performance of the sensor.

Chemical composition should be analyzed since the goal is to fabricate PZT with composition of 52% $PbZrO_3$ and 48% $PbTiO_3$. Energy-dispersive X-ray spectrum (EDS), which is an element analysis, can be used for chemical composition analysis. EDS stimulates the emission of characteristic X-ray from a sample. Because all elements have their own unique atomic structure, the energy of their characteristic X-ray spectrum can be used for determination of elements contained and percentage of each element contained in the sample, which can be calculated the chemical composition.

Mechanical properties may not be easy to analysis when it is still in the form of nanoparticles. However, after PZT film fabrication, nano-indentation should be done to determine mechanical properties. Nano-indentation is a hardness testing tool. It can be used to identify hardness of the sample and calculate young's modulus with assumption of the film is linear and isotropic.

Electrical properties should be measured after the film fabrication procedure is determines and set. Resistant, capacitance, and impedance should be measured by an impedance analyzer. Ferroelectric Hysteresis measurement and analysis should be prepared to having better understand of the material. Hysteresis loop measures polarizing behavior of a material under symmetrically applied positive and negative field. Remnant polarization and coercive field can be determined by the hysteresis loop, also called P-E loop. These two factors are indications of ferroelectric properties. Remnant polarization shows the stability of polarization. High remnant polarization means higher energy density of a material. Coercive field determines poling

capability. High coercive field means stronger resistant on depolarization. Therefore, for sensor application purpose, high remnant polarization and high coercive field are desirable.

5.3 Ink and film

There are three basic requirements for ink fabrication. One is it needs to have good wettability on a choice of substrates. If wettability is not good, the ink will not be able to bind with the substrate and form a strong film. Second one is that PZT nanoparticles need to stay in suspension in the ink. Third one is that an ink formula needs to be compatible to a choice of printing systems and to the substrate. If the ink contains chemicals that are not compatible to the printing system or the substrate, it could damage the system or substrate. Therefore, ink fabrication techniques and ink compositions should be studied to determine the best choice for the chosen system and substrate.

After the ink is properly fabricated, PZT film can be fabricated. The requirements for PZT films can vary depend on the applications. However, there are two universal requirements for PZT film—strong and dense. Then, after PZT films are prepared, measurements on mechanical properties, electrical properties, performance of the sensor should be analyzed.

References

[1] Tianming Wang and Brian Derby. "Ink-Jet Printing and Sintering of PZT." Journal of American Ceramic Society 88, Vol. 8, pp. 2053-2058 (2005)

[2] K. Sivanandan, Asha T. Achuthan, V. Kumar, Isaku Kanno. "Fabrication and transverse piezoelectric characteristics of PZT thick-film actuators on alumina substrates" Sensor and Actuators A: Physial, 148, pp. 134-137 (2008)

[3] Tomokazu Tanase, Yoshio Kobayashi, and Mikio Konno. "Preparation of lead zirconate titanate thin films with a combination of self-assembly and spin-coating techniques." Thin Solid Films, Vol. 457, pp.264-269 (2004)

[4] Sung-Gap Lee. "Effects of sol infiltration on the screen-printed lead zirconate titanate thick films." Materials Letters 61, pp. 1982-1985 (2007)

[5] Chun-Hung Hsueh and Chia-Che Wu. "Fabrication of lead zirconium titanium silica composite films on copper/polymide flexible substrates." Smart Material Structure, No. 19 (2010)

[6] PI Ceramic. (Piezotechnology). "Piezo Manufacturing Technology." (http://www.piceramic.com/piezo_technology.php>.

[7] Chun-Hung Hsueh and Chia-Che Wu. "Fabrication of lead zirconium titanium silica composite films on copper/polymide flexible substrates." Smart Material Structure, No. 19 (2010)

[8] Sang Yup Kim, Toshio Tanimoto, Kenji Uchino, Chan Hee Nam, Sahn Nam, and Woo II Lee. "Effects of PZT particle-enchanced ply interfaces on the vibration damping behavior of CFRP composites." Composites: Part A 42, pp. 1477-1482 (2011)

[9] Ronald Staut, Brain Julius, and John Meiman. "PZT Powder Manufacturing" <www.ceramicindustry.com> (2010)

[10] Q.Z. Cao and Y. Wang. Nanostructures and Nanomaterials: Synthesis, Properties, and Applications, Word Scientific Series in Nanoscience and Nanotechnology, Ch2-3

[11] B. Su, T.W. Button, C.B. Ponton. "Control of the particle size and morphology of hydrothermally synthesized lead zirconate titanate powders." Journal of Materials Science 39, pp. 6439-6447 (2004)

[12] Yuan Deng, Li Liu, Yue Cheng, Ce-Wen Nan, Shu-jing Zhao. "Hydrothermal synthesis and characterization of nanocrystalline PZT powders." Elsevier Science. Materials Letters 57, pp.1675-1678 (2003)

[13] S.F. Wang, Y.R. Wang, T. Mahalingam, J.P. Chu, and K.U. Lin. "Characterization of hydrothermally synthesized lead zirconate titanate (PZT) ceramics." Materials Chemistry and Physics 87, pp.53-58 (2004)

[14] Scott Harada, Steve Dunn. "Low temperature hydrothermal routes to various PZT stoichiometries." Springer 2007. Journal Electroceram 20:65-71 (2008)

[15] Maria Traianidis, Christian Courtois, Anne Leriche, and Bernard Thierry. "Hydrothermal Synthesis of Lead Zirconium Titanate (PZT) Powders and their Characteristics. Journal of the European Ceramic Society, No. 19, pp. 1023-1026 (1999)

[16] R.N. Das and P. Pramanil. "In Situ Synthesis of Nanosized PZT powders in the Precursor Material and the Influence of Pzrticle Size on the Dielectric Property." Nanostructured Materials. Vol.10, No.7, pp. 1371-1377 (1998)

[17] Zhong-Cheng Qiu, Jia-Ping Zhou, Gangqiang Zhu, Peng Liu, and Xiao-Bing Bian. "Hydrothermal synthesis of Pb(Zr0.52Ti0.48)O3 powders at low temperature and low alkaline concentration. Bulletin Materials Sciences, Vol. 32, No. 2, pp. 193-197 (2009)

[18] M.S. Vijaya. Piezoelectric Materials and Devices: Applications in Engineering and Medical Sciences. Florida. CRC Press. Taylor & Francis Group, Ch1-3. (2013)

[19] K. Byrappa, T. Ohachi (Eds). B.L. Gersten. Crystal Growth Technology. "Growth of Muticoponent Perovskite Oxdie Crystals: Synthesis Conidtions for the Hydrothermal Growth of Ferroelectric Powders." New York. William Andrew Inc. Springer. pp.300-333 (2001)

[20] K. Byrappa and Masahiro Yoshimura. Handbook of Hydrothermal Technology—A Technology for Crystal Growth and Materials Procesing. New York. Noyes Publications. pp. 164-184 (2001)

[21] Seung-Beom Cho, Magdalenda Oledzka, and Richard E. Riman. "Hydrothermal synthesis of acicular lead zirconate titanate (PZT)." Journal of Crystal Growth. No. 226, pp. 313-326 (2001)